Journal of Luminescence xxx (xxxx) xxx–xxx

Contents lists available at ScienceDirect

Journal of Luminescence

journal homepage: www.elsevier.com/locate/jlumin

Broadband near-infrared luminescence at around 1.0 μm in Pr^{3+}/Er^{3+} co-doped tellurite glass

Minghan Zhou, Yaxun Zhou*, Yarui Zhu, Xiue Su, Jun Li, Hanru Shao

College of Information Science and Engineering, Ningbo University, Zhejiang 315211, China

ARTICLE INFO

Keywords:
Tellurite glass
Pr^{3+}/Er^{3+} co-doping
Broadband emission
1.0 μm band

ABSTRACT

In this work, the near-infrared band photoluminescence properties around 1.0 μm in Pr^{3+}/Er^{3+} co-doped tellurite glass was investigated. The doped tellurite glass with composition TeO_2-WO_3-ZnO-La_2O_3 was synthesized using melt-quenching technique and characterized by UV/Vis/NIR absorption spectrum, near-infrared emission spectrum, X-ray diffraction (XRD) pattern and Raman spectrum. Under the excitation of 488 nm laser, a broad 1.0 μm band luminescence ranging from 950 to 1100 nm with a full width at half maximum (FWHM) up to 94 nm was observed, nearly two times compared to that in Pr^{3+} or Er^{3+} single-doped case. This broadband near-infrared luminescence was contributed by the Er^{3+}:$^4I_{11/2} \rightarrow {}^4I_{15/2}$ and Pr^{3+}:$^1D_2 \rightarrow {}^3F_4$ radiative transitions which lead to two emissions located at 980 and 1040 nm, respectively. The structural analysis of XRD pattern and Raman spectrum proved the long-range structural disorder in synthesized glasses, and based on the absorption spectrum, some important spectroscopic parameters such as the Judd-Ofelt intensity parameter, spontaneous radiative transition probability, fluorescence branching ratio, absorption and emission cross-sections, and gain coefficient spectrum were calculated to reveal the radiative properties of doped tellurite glass. The obtained results indicate that Pr^{3+}/Er^{3+} co-doped tellurite glass is a promising candidate to fabricate a broadband near-infrared luminescent source for telecommunication and other applications such as medical imaging system.

1. Introduction

The near-infrared band lasing sources have been extensively investigated during the last decades and they continue to attract a considerable interest because of their important applications in many fields, such as optical communication, high-density optical storage, solar cell, remote sensing, lasing radar, medical diagnostics and so on [1–4]. For instance, a broadband near-infrared lasing output around 1.0 μm is essential for medical imaging, since in the operation of optical coherence tomography (OCT), a broader lasing emission spectrum contributes to a higher axial resolution of the OCT image. Additionally, an emission centered at around 1.0 μm is beneficial to obtain a large imaging depth in aqueous tissues because of its weak optical absorptions of hemoglobin and water in a biological sample [5,6].

So far, trivalent rare-earth ions are undoubtedly the most important activators for achieving this class of lasing sources. Among them, Er^{3+}, Yb^{3+}, Pr^{3+} and Nd^{3+} have been proved to exhibit lasing emissions in the near-infrared band around 1.0 μm for scientific and technological interest through the radiative transitions of Er^{3+}:$^4I_{11/2} \rightarrow {}^4I_{15/2}$, Yb^{3+}:$^2F_{5/2} \rightarrow {}^2F_{7/2}$, Pr^{3+}:$^1D_2 \rightarrow {}^3F_{4,3}$ and Nd^{3+}:$^4F_{3/2} \rightarrow {}^4I_{11/2}$, respectively [7–10]. For example, Franczyk et al. reported a Yb^{3+}-doped phosphate glass single-mode fiber laser with slope efficiency of 66.6% and output power of 11.6 W at 1.0 μm by using a 4 cm-long fiber [11], and Wang et al. reported a 15.5 W laser output at 1064 nm over a fiber length of 25 cm with slope efficiency of 57% by using a photonic crystal fiber containing seven different Nd^{3+}-doped single-mode cores [12]. However, the spectral bandwidth especially the spectral flatness from these lasing emissions is unsatisfactory in the rare-earth single-doped case, which is indispensible in optical communication, tunable lasers and other applications requiring broadband source.

In this paper, Pr^{3+}/Er^{3+} co-doped tellurite glass was synthesized and the structural and luminescence properties were investigated. The investigated glass generates a broadband and flat near-infrared emission in the range of 950–1100 nm with a full width at half maximum (FWHM) up to 94 nm under the excitation 488 nm laser, which is reported for the first time to our best knowledge. In the present work, tellurite glass was selected as the glass host due to its excellent properties such as wide transparency in a broad wavelength range of 0.35–6 μm, large rare-earth ion solubility which is 10–50 times larger than in silica glass, low host phonon energy (~750 cm^{-1}) among oxide

* Corresponding author.
E-mail address: zhouyaxun@nbu.edu.cn (Y. Zhou).

https://doi.org/10.1016/j.jlumin.2018.07.021
Received 20 April 2018; Received in revised form 23 June 2018; Accepted 18 July 2018

glasses, good mechanical stability and corrosion resistance compared with non-oxide glasses [13,14].

2. Experimental details

Pr^{3+} single- and Pr^{3+}/Er^{3+} co-doped tellurite glasses were prepared from high-purity TeO_2, WO_3, ZnO, La_2O_3, Pr_6O_{11} and Er_2O_3 powders by applying conventional melt-quenching technique. The investigated glasses are composed of $70TeO_2$-$10WO_3$-10ZnO-$10La_2O_3$ in mole percent and doped with 0, 0.3, 0.6, 1 wt% varied amount of Er_2O_3 and 1 wt% fixed amount of Pr_6O_{11}, which are hereafter labeled as P1E0, P1E03, P1E06 and P1E1, respectively. The precision weighed and well mixed 10 g batches of raw materials were preheated in an alumina crucible at 200 °C for 15 min before melted in an electric furnace at 950 °C for 45 min. During the melting, the high temperature glass melt was stirred at every 15 min to remove the gas bubble and get more homogeneous sample. After that the glass melt was rapidly poured into a preheated brass mold to avoid thermal shock and annealed at 345 °C for 2 h below the glass transition temperature to release mechanical stress, then cooled slowly down to the room temperature at a rate of 10 °C/h. As a comparison, Er^{3+} single-doped tellurite glass with 1 wt% amount of Er_2O_3 was also prepared and denoted as P0E1. The all obtained glass samples were finally polished and cut into the same thickness with 1.5 mm for physical and spectroscopic measurement.

Glass density was measured based on the Archimede's principle using distilled water as an immersed liquid. Refractive index was measured using a prism coupler (Sairon Tech-SPA4000 TM) at a wavelength 632.8 nm. Powder X-ray diffraction (XRD) pattern was recorded using a power diffractometer with Cu Ka radiation (40 kV25 mA) and a graphite monochromator. Raman spectrum was recorded in a Horiba Jobin Yvon HR800 Raman spectrometer with a 785 nm laser excitation source. Absorption spectrum in the spectral range of 400–2200 nm was measured by a Perkin Elmer Lambda 900 UV/VIR/NIR spectrophotometer. Fluorescence emission spectrum ranging from 800 to 1350 nm was measured by a computer-controlled TRIAX 320 fluorescence spectrometer (Jobin-Yvnon Crop) under the pump of 488 nm laser. All the above physical and spectroscopic measurements were performed at room temperature and some measured physical parameters were listed in Table 1.

3. Results and discussion

3.1. XRD pattern and Raman spectrum

The measured XRD patterns of Pr^{3+} single-doped (P1E0) and Pr^{3+}/Er^{3+} co-doped (P1E03) tellurite glasses (chosen as a representative) are displayed in Fig. 1. It is found that the diffractogram of the synthesized glasses are similar in shape with a broad hump between 20° and 40° (peak at about 29°) but the absence of any detectable sharp discrete diffraction peaks, indicating the presence of long-range structural disorder i.e. amorphous state nature for the synthesized glasses [15,16].

The Raman spectra depicted in Fig. 2 exhibit the broad peaks which are also attributed to the disorder of glass structure. Among them, the peak located at about 328 cm^{-1} is associated with the symmetrical stretching or bending vibrations of Te-O-Te or O-Te-O linkages at

Table 1
The density (ρ), refractive index (*n*), Pr^{3+} concentration (N_{Pr}) and Er^{3+} concentration (N_{Er}) of the prepared glasses.

Samples	ρ (g/cm^3)	*n*	N_{Pr} (×10^{20} / cm^3)	N_{Er} (×10^{20} / cm^3)
P1E0	5.608	2.013	0.6545	0
P1E03	5.639	2.014	0.6581	0.5309
P1E06	5.697	2.018	0.6649	1.0695
P1E1	5.684	2.016	0.6634	1.7714
P0E1	5.583	2.011	0	1.7399

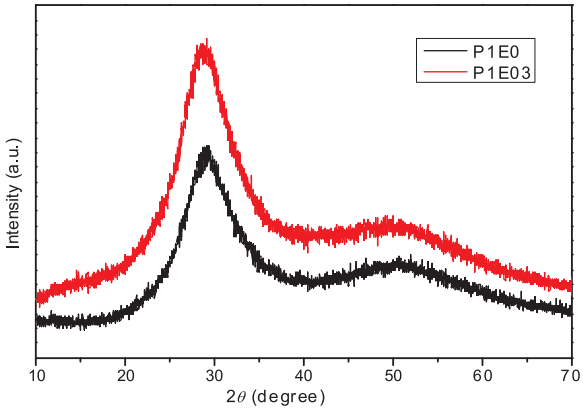

Fig. 1. The XRD patterns of Pr^{3+} single-doped and Pr^{3+}/Er^{3+} co-doped tellurite glasses.

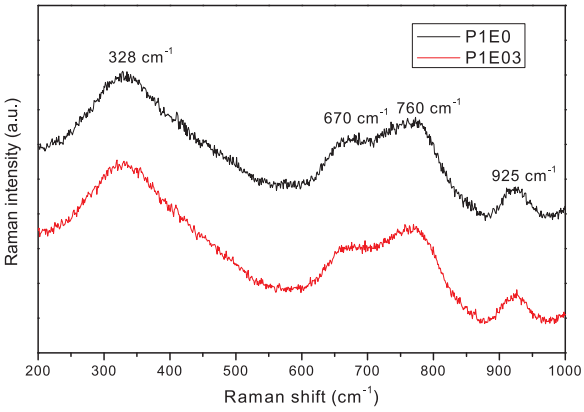

Fig. 2. The Raman spectra of Pr^{3+} single-doped and Pr^{3+}/Er^{3+} co-doped tellurite glasses.

corner sharing sites along the chains of TeO_4, TeO_3 and TeO_{3+1} polyhedra, the shoulder at 670 cm^{-1} is related to the antisymmetric stretching modes of Te-O-Te linkages, made up of two unequivalent Te-O bonds (one equatorial oxygen and the other axial) in the TeO_4 structural units, the band located at 760 cm^{-1} is ascribed to the stretching vibrations of Te-O bonds in TeO_3 trigonal pyramid (tp) which result from the transformation of the TeO_4 or from intermediate TeO_{3+1} polyhedra, while the band at 925 cm^{-1} is due to the stretching vibrations of W-O^- and/or W=O in the tetrahedral [WO_4] units or octahedral [WO_6] units [17–19].

3.2. Absorption spectrum and Judd-Ofelt analysis

Fig. 3 displays the absorption spectra of Pr^{3+} single-, Er^{3+} single- and Pr^{3+}/Er^{3+} co-doped tellurite glasses in the 400–2200 nm wavelength range at room temperature. All the absorption bands due to the electronic transitions from the ground states to their respective excited states of Pr^{3+} and Er^{3+} are labeled. Among them the bands centered at 1948, 1533, 1440, 1012, 594, 487, 472 and 447 nm are ascribed to the absorption transitions from the ground state $^3H_4$ of Pr^{3+} to the excited states $^3F_2$, $^3F_3$, $^3F_4$, $^1G_4$, $^1D_2$, $^3P_0$, $^3P_1$ and $^3P_2$ respectively [17,20], while those of bands centered at 1532, 976, 798, 652, 543, 522 and 488 nm are attributed to the absorption transitions from the ground state $^4I_{15/2}$ of Er^{3+} to the excited levels $^4I_{13/2}$, $^4I_{11/2}$, $^4I_{9/2}$, $^4F_{9/2}$, $^4S_{3/2}$, $^2H_{11/2}$ and $^4F_{7/2}$ respectively [21]. With the increase of Er^{3+} doped concentration, it is found that the intensities of Er^{3+} absorption peaks increase accordingly but the peak positions of all absorption bands hardly change, indicating the doped rare-earth ions are homogeneously distributed in glass matrix. Meanwhile, it is worth to mention that the absorption